AD A126782

DTIC ELECTE APR 13 1983 D

Accession For
NTIS GRA&I ☒
DTIC TAB ☐
Unannounced ☐
Justification

By
Distribution/
Availability Codes
Dist | Avail and/or Special
A | 21

Network oxygen exchange during water diffusion in SiO_2

Robert Pfeffer
US Army Electronics Technology and Devices Laboratory (ERADCOM), Fort Monmouth, New Jersey 07703

Milton Ohring
Stevens Institute of Technology, Hoboken, New Jersey 07030

(Received 26 July 1979; accepted for publication 5 October 1979)

In an investigation of the mechanism responsible for the transport of water through SiO_2 thin films, we have performed tracer diffusion measurements involving network ^{18}O demonstrating the importance of oxygen exchange between the SiO_2 network and molecularly dissolved water. We have found that in the presence of water, bound network oxygen diffuses through SiO_2 as a constituent of molecularly dissolved water. Employing methods common to state-of-the-art semiconductor technology, the central region within a thermal oxide layer grown on silicon was enriched with immobile ^{18}O by ion implantation. After heating in atmospheres with different water contents, the extent of ^{18}O diffusion was determined by observing changes in the concentration profile of implanted ^{19}O by means of nuclear resonance profiling making use of the 629-keV resonance of the $^{18}O(p,\alpha)\,^{15}N$ reaction. Diffusions conducted in steam at 1 atm (at temperatures as low as 250 C) showed an activation energy of about 17 kcal/mol, which is close to that originally measured for water permeation in SiO_2. Diffusions in both air and dry nitrogen showed a similar activation energy, with respective pre-exponential factors two and three orders of magnitude below the steam value. Diffusion in low-pressure water vapor showed a clearly linear dependence on gas phase water concentration down to 80 ppm. These results are consistent with a model of water diffusion in SiO_2 in which the diffusion mechanism is the interstitial transport of dissolved molecular water accompanied by a reversible reaction with silicon-oxygen bonds in the network.

PACS numbers: 66.30. – h, 81.60.Dq

I. INTRODUCTION

The formation of thin insulating films on the surface of semiconductor materials is an important part of modern electronic technology. Because of its commercial importance, various means of film growth have been intensively studied,[1] especially for high-quality gate insulators on silicon surfaces. For that application a more or less standard practice of thermal oxidation in dry oxygen or steam atmospheres has evolved, by which oxide films are routinely produced satisfying the stringent requirements of integrated circuit devices. However, the ever-increasing complexity and operating speed of such devices requires ever smaller and more closely packed component structures. The scale of sizes has now reached a point where basic changes are required in manufacturing methods. For example, the need is foreseen to hold temperatures in all steps of a processing sequence low enough to prevent significant migration of dopants. Virtually all of the many studies of thermal oxidation have been device oriented. Physical models of the oxidation process have received little attention, especially for steam oxidation; only now are models being tested with sufficient care to generate a consensus of acceptance. For the future, a greater understanding of the mechanism responsible for oxidation in the presence of water is imperative, especially in the new low-temperature regime, where it now appears that processing of the coming generation of devices will take place.

The main object of our work is to clarify the mechanism of SiO_2 film growth in atmospheres containing water. Through determination of the kinetics of network oxygen exchange, we provide a direct experimental demonstration of the validity of a recently proposed model of the oxidation process.[2] According to this model, growth proceeds by inward interstitial diffusion of dissolved molecular water, which simultaneously reacts with the SiO_2 network to form immobile reaction products. In order to accomplish this, we apply the technique of ion implantation to measuring tracer oxygen diffusion in SiO_2. Using this technique, the central region within a thermal oxide layer grown on silicon is enriched with immobile ^{18}O. After heating in atmospheres with different water contents, the extent of ^{18}O diffusion is determined by observing changes in the concentration profile of implanted ^{18}O by means of nuclear resonance profiling[3] making use of the 629-keV resonance of the $^{18}O(p,\alpha)$ ^{15}N reaction. The observation of tracer distribution broadening both eliminates surface effects and enhances the sensitivity of diffusion measurements, enabling tracer diffusion measurements to be carried out at considerably reduced temperatures and ambient gas-phase concentrations.

II. MODELS OF OXIDATION AND DIFFUSION

Various tracer experiments, cited by Deal and Grove,[4] have established that the thermal oxidation of silicon proceeds by the inward transport of oxygen through the oxide layer as a constituent of molecularly dissolved oxygen or water. The silicon substrate is converted to new oxide by the incorporation of atomic oxygen at the oxide-silicon interface after molecular dissociation. The layer thickens by formation of new oxide underneath the existing layer.

DTIC FILE COPY

 0021-8979/81/020777-08$01.10 © 1981 American Institute of Physics

83 04 12 081

There is much evidence that dry thermal oxide layers formed on silicon surfaces have the same structure as vitreous silica. X-ray diffraction experiments showed the oxide layers to be amorphous.[5] The density of the layers is close to that of fused silica[6] as are the changes in density induced by ionizing radiation.[7] The optical properties are essentially identical,[8] as are the Si-O-Si bond angles obtained from electron diffraction and IR absorption experiments.[9]

The mechanism of oxygen diffusion through SiO_2 is now generally believed to be the interstitial transport of dissolved molecular oxygen. The process occurs without any direct bonding between the diffusing species and the SiO_2 network; it rather involves the transport of nonreacting molecules through the interstices or cavities in the network. This interstitial model was first proposed by Anderson and Stuart[10]; they calculated the activation energy for diffusion as the elastic energy required to deform the network by enlarging the circular doorways between interstices enough for the diffusing species to pass. An essential feature of this model is a lack of chemical binding between the diffusing species and the network.[11] Although the model is simplistic, the functional dependence of activation energy upon molecular diameter agrees well with activation energies measured for molecular diffusion of various gases in fused silica (Ref. 12, p. 42). It is also consistent with the linear dependence of diffusivity upon ambient pressure observed by Norton[13] for oxygen in vitreous silica, whose diffusion is not accompanied by any significant reactions with the SiO_2 network. This was demonstrated recently in a tracer experiment[14] in which thermal oxide films which were grown in natural oxygen were further grown in ^{18}O-enriched gas. Almost all additional ^{18}O was observed to collect in a layer at the Si-SiO_2 interface, while less than 0.3% remained in the previously grown region. Great care was taken to eliminate any water in this experiment.

The mechanism for water diffusion through SiO_2 is similarly thought to involve the interstitial transport of dissolved molecular water.[2] The transport of the diffusing species, dissolved molecular water, is again postulated to involve no direct reaction with the network. However, the permeation of water in SiO_2 involves a strong reaction with silicon-oxygen bonds in the network, in which the molecularly dissolved water dissociates to form two OH units with the additional O ion being provided by the SiO_2 network.[2,15] This reversible reaction

$$H_2O + Si\text{-}O\text{-}Si \rightleftharpoons 2\ SiOH \quad (1)$$

leads to equilibrium concentrations of reaction products which are large compared to that of molecularly dissolved water, and which depend on the square root of ambient water vapor concentration, in agreement with measurements of water solubility in vitreous silica.[16] The reaction products (i.e., SiOH groups) are postulated to be immobile; only the molecularly dissolved water diffuses.

In the present study, it was found that the reaction between dissolved molecular water and the SiO_2 network acts to remove previously immobile implanted ^{18}O from its network site and to convert it instead to a constitutent of a mobile species. In the context of this model, that species is molecular water and the exchange proceeds via the reaction

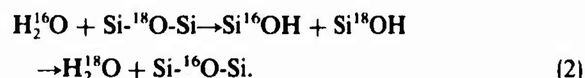

$$H_2^{16}O + Si\text{-}^{18}O\text{-}Si \rightarrow Si^{16}OH + Si^{18}OH \rightarrow H_2^{18}O + Si\text{-}^{16}O\text{-}Si. \quad (2)$$

The tracer ^{18}O was observed to diffuse through SiO_2 layers with a diffusivity which was linearly proportional to the partial pressure of ambient water vapor, and with an activation energy of diffusion which matched those previously measured for water,[16] even in atmospheres containing far larger concentrations of oxygen. In the absence of ambient water vapor, no diffusion could be detected.

III. EXPERIMENTAL PROCEDURE

A. Materials preparation

The SiO_2 layers were formed by thermal oxidation of 2-in.-diam single-crystal silicon wafers obtained from Monsanto Corporation; they were of (100) orientation, with one face polished; their resistivity was 4 Ω cm (n type). They were degreased, cleaned, and oxidized to 2000 Å in flowing dry oxygen at 1 atm at 1200 C. ^{18}O in the form of isotopically enriched gas (70 at. %, obtained from ProChem Isotopes) was then implanted into the SiO_2 films to a fluence of 3×10^{15} ions/cm^2. To avoid $H_2^{16}O$ contamination the mass analyzer was set at 36 amu; the accelerating voltage was 80 kV. The resulting ^{18}O concentration profile was an Edgeworth distribution centered at 768 Å with a standard deviation of 283 Å and a third-moment ratio of -0.164 (Ref. 17). A mass analysis of the residual gas within the ion implantation apparatus showed the major contaminants to be (^{16}O-^{18}O), ($^{15}N)_2$, and ^{40}Ar, in quantities insufficient to affect the fluence measurement significantly. The wafers received no immediate postimplant treatment. Samples were prepared by cleaving the oxidized and implanted wafers into sections which had been individually marked to indicate their original locations on the wafers.

B. Thermal treatments

The thermal treatments, which involved heating samples in atmospheres containing various water vapor concentrations, were carried out in order to determine both the activation energy of tracer ^{18}O diffusion as well as its functional dependence upon ambient vapor phase concentration. The former was determined by observing the temperature dependence of the tracer diffusivity in a particular atmosphere; the latter by observing its dependence on H_2O pressure at a single temperature.

1. Temperature dependence

The first set of thermal treatments was carried out in room air. The room was maintained at a temperature of 21 C and a relative humidity of 50%. Samples were placed in a horizontal tubular alloying furnace, lined with a fused quartz diffusion tube and open at one end; their temperatures were monitored by means of a thermocouple which was inserted in the diffusion tube at the sample location.

Treatments were carried out by loading a batch of samples on a preheated fused quartz carrier; sample manipulation involved withdrawing the carrier from the furnace for no more than 30 s per operation. Temperatures ranged from 413 to 789 C and durations from 3540 to 230 800 s. Another set of treatments was carried out in dry N_2 at 1 atm in an identical manner. Gas was obtained via boiloff of liquid nitrogen; flow was 500 cc/min (equivalent at 70 °F, 1 atm). Temperatures ranged from 543 to 1160 C and durations from 10 980 to 1 799 210 s. A similar procedure was followed for thermal treatments in steam at 1 atm. The steam was generated by boiling deionized water in a stoppered flask. The boiling rate was governed by a variable autotransformer supplying power to a hemispherical heating mantle around the flask. Steam was conducted to the narrowed end of the diffusion tube through a horizontal pyrex tube emerging from the neck of the flask. The entire length of horizontal tubing and the neck of the flask were wrapped in fiberglass heating tape and maintained at a temperature of 120 C to avoid condensation. An antibackstreaming plug formed by a wad of fiberglass tape around the thermocouple tube allowed a slight positive pressure to be maintained in the furnace. Temperatures ranged from 263 to 619 C and durations from 1290 to 85 400 s.

2. Pressure dependence

A set of thermal treatments was carried out in pure water vapor at reduced pressures; these were performed within the bell jar of a vacuum evaporation station. The samples were placed within a section of quartz tubing, as was a thermocouple. The tubing was then inserted into a small tubular resistance furnace, whose pedestal mount rested on the baseplate. Electrical power for the furnace was supplied by a variable autotransformer through feedthroughs in the baseplate; roughly 80 W was required to maintain a sample temperature of 800 C. No difficulty was encountered in keeping the temperature constant to within ± 3 C by manually adjusting the autotransformer voltage. Water vapor was supplied by evaporation of deionized water in a stoppered vacuum flask; a continuous flow was maintained by exhausting the chamber with a mechanical forepump through a choked down roughing valve. Vapor pressure was regulated by manually adjusting both the roughing valve and a micrometer-type variable leak valve in the supply line; pressure excursions on the longer runs amounted to no more than 20% of the average value. Temperatures ranged from 740 to 842 C, durations from 7200 to 609 000 s, and pressures from 0.062 to 8.9 Torr.

In addition to these treatments, several samples were treated in high vacuum (10^{-6} Torr) in order to assess the substitutionality of the implanted ^{18}O and the extent of damage to the oxide. One was maintained at 815 C for 579 600 s; another at 690 C for 230 400 s, following which it received a dry nitrogen treatment at 1150 C for 11 400 s.

C. Nuclear resonance profiling

In order to determine the extent of ^{18}O diffusion induced by the thermal treatments, alpha particle yield curves were taken using the method of nuclear resonance profiling.[3] The energy of a beam of protons from a 2-MeV Van de Graaff electrostatic accelerator (Model A, High Voltage Engineering Corp.) was systematically stepped in the neighborhood of the 629-keV resonance in the $^{18}O(p,\alpha)^{15}N$ reaction. Beam energy was monitored by means of an NMR gaussmeter whose probe was mounted between the analyzing magnet pole shoes; excursions in the magnetic field were easily kept small enough to limit beam energy variations to under ± 40 eV during a typical 1.5–2 min duration alpha particle count. The detector was a silicon surface barrier device (25-mm^2 area, 100-μm depletion depth) at an angle of 150° to the beam direction, shielded from backscattered protons by a 1.3-mg cm^{-2} polyester foil. Samples were mounted normal to the beam and biased to collect secondaries. Each batch of samples profiled included a reference sample that had been ^{18}O implanted but not thermally treated; the reference samples provided a continuous self-calibration for the proton beam energy. An additional calibration was performed by means of (p,γ) nuclear resonance profiling of thick targets containing uniform concentrations of appropriate nuclides. This was done primarily to determine the spread (i.e., the distribution of proton energies) in the incident beam.

The alpha particle counts at each beam energy accumulated on a scaler until the proton fluence on the sample had reached a preset value (typically 50 μC). Alpha particle counts ranged from 1000 to 5000 per run; background counts were negligible. Beam current was held to 0.5 μA to avoid heating the samples. The range of beam energy settings spanned was typically 13 keV on either side of the energy at which the alpha yield was maximum, corresponding to a distance of 2100 Å on either side of the distribution peak.[18]

IV. RESULTS AND ANALYSIS

The raw data obtained by the nuclear resonance profiling consisted of an alpha particle yield curve for each sample. A representative set of these curves appears in Fig. 1, in

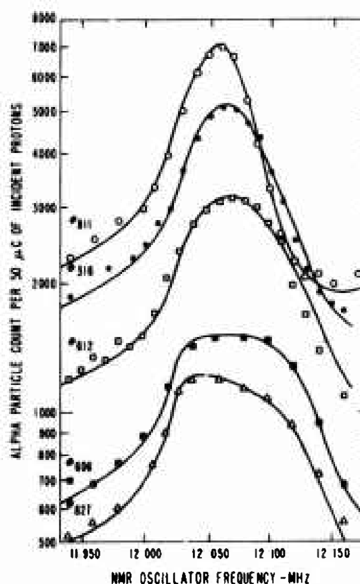

FIG. 1. Observed alpha particle yield curves for selected samples. Continuous curves represent calculated yield curves.

which the different symbols denote data recorded for the samples indicated. For the two lowest curves the counting time was doubled to obtain sufficient statistical accuracy: the points plotted for those curves are half the recorded counts. Also shown with each observed curve is a theoretically derived curve (the continuous curve between the data points); these were calculated according to the procedure described in the following section.

A. Method of determining ^{18}O tracer diffusivity

As discussed below, the implantation process caused ^{18}O to effectively replace existing oxygen as a constituent of the SiO_2 network. According to the model of diffusion described in Sec. II, the exchange of network oxygen with dissolved molecular water is solely responsible for any observed change in the distribution of implanted ^{18}O. The dependence of the tracer ^{18}O diffusion on thermal treatment parameters is a diagnostic of the mechanism of water diffusion in SiO_2 layers, and a test of the validity of this model.

The analysis of tracer ^{18}O transport via the exchange reaction involves three interrelated diffusion coefficients. The first of these, D_{eff}, is the quantity normally measured in permeation experiments. This effective diffusivity is independent of ambient gas-phase concentration only if the fluxes of emerging particles and dissolved species have the same pressure dependence. (Such is not the case for water diffusion, where D_{eff} is the apparent diffusivity of reacted water.) The transport of the actual mobile species is described by the microscopic diffusivity D. For a dilute gas in a spatially uniform network, D is independent of ambient gas-phase concentration, spatial location, and dissolved gas concentration; it depends only on temperature. For oxygen diffusion in SiO_2, which proceeds without appreciable dissociation or reaction with the network, D_{eff} and D have the same value. However, for water diffusion they are related by the equation

$$D_{eff} = D\,2[H_2O]/(2[H_2O] + [SiOH]). \quad (3)$$

The fraction represents the probability that any particular OH group will be part of a diffusing water molecule; the factor of 2 accounts for the removal of two OH groups from the network by each water molecule. The effective diffusion of tracer ^{18}O by means of the exchange reaction is described by the tracer diffusivity D^*. In the presence of free exchange under quasisteady conditions, D^* is related to D by the equation

$$D^* = D[H_2O]/(2[SiO_2] + [H_2O] + [SiOH]). \quad (4)$$

The fraction is the probability that an ^{18}O will be part of a diffusing water molecule. The factor of 2 accounts for the incorporation of two oxygen atoms per SiO_2 molecule.

The value of D^* characteristic of a given thermal treatment is reflected in the change of the implanted ^{18}O distribution resulting from the treatment. Once the alpha particle yield is measured, the extent of change is in principle determinable by inversion of the integral equation for the yield, namely,

$$Y(E_b) = \int_0^{x_0} dx\rho(x,t) \int_0^{\infty} dE_i g(E_b,E_i) \times \int_0^{E_i} dE \frac{d\sigma}{d\Omega}(E) f(E,E_i,x), \quad (5)$$

where E_b is the mean energy of the incident proton beam, E is the energy of reacting protons, E_i is the normal energy of protons incident on the surface of the layer, x_0 is the thickness of the oxide layer, x is the depth at which the reaction occurs, $\rho(x,t)$ is the ^{18}O concentration profile (i.e., atoms per unit volume at depth x at time t), $d\sigma/d\Omega$ is the differential cross section of the $^{18}O(p,\alpha)\,^{15}N$ reaction, $g(E_b,E_i)dE_i$ is the fraction of protons in the beam which have an incident between E_i and $E_i + dE_i$, and $f(E,E_i,x)dE$ is the probability that a proton which has started with energy E_i and arrived at depth x will have an energy between E and $E + dE$.

If the functions $g(E_b,E_i)$, $f(E,E_i,x)$, and $d\sigma/d\Omega(E)$ are all previously known and the yield $Y(E_b)$ is observed, then the function $\rho(x)$ can in principle be determined by inversion of the integral equation. An enlightening discussion of this matter appears in Ref. 19, in which a similar calculation [involving the $^{27}Al(p,\gamma)\,^{28}Si$ reaction] was done.

In practice, deconvolution is a complicated procedure, entailing large errors whose propagation is difficult to track. However, once the initial ^{18}O distribution is determined, its subsequent evolution is predictable through macroscopic diffusion theory provided the properties of the medium are correctly perceived and the proper boundary conditions are applied. This is treated further in the Appendix, where the evolved distribution is calculated as a functional of the product D^*t (t being the duration of treatment). Based on this distribution together with the other constituent functions of the yield integral given in the Appendix,[20] the yield was calculated for each of a number of discrete values of D^*t. The resulting family of yield curves, which is illustrated in Fig. 2, was compared to the experimental yield curve resulting from that thermal treatment. The appropriate value of D^*t was

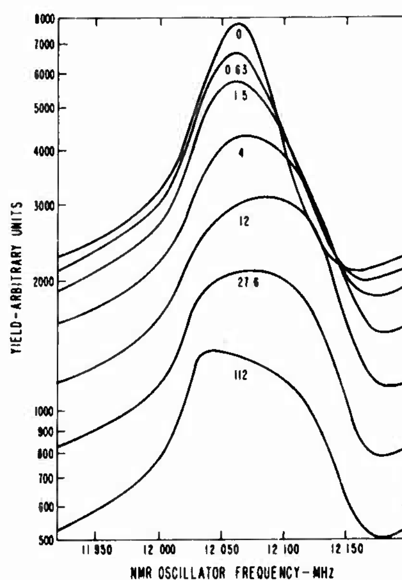

FIG. 2. Calculated alpha particle yield curves. Labels indicate D^*t, in units of $\sigma^2_{implant}$.

taken as that which indexed the calculated yield curve most closely matching the experimental yield curve.

For routine measurements of D^*, a procedure was adopted which allowed shorter thermal treatments and also greatly shortened the time spent in nuclear profiling. It can be seen from the family of theoretical yield curves in Fig. 2 that the peak yield of alpha particles can be regarded as a monotonically decreasing function of D^*t. This function was constructed by calculating a large number of theoretical alpha particle yield curves. The peak value of each of those curves was tabulated along with the value of D^*t associated with the curve; those values were then connected with a smooth curve. To determine the proper value for a given thermal using this function, it was necessary to measure an alpha particle yield curve for a sample only in the vicinity of its peak so as to determine the peak yield. This quantity was then normalized to that of a reference sample located nearby on the wafer. The appropriate value of D^*t was then found simply by locating the resulting peak yield ratio on a graph of that function.

B. Temperature and pressure dependence of tracer diffusivity

The temperature dependence of D^* was determined as follows. First, D^* was calculated from the observed data using the methods described in the previous section. For each of the three atmospheres (i.e., steam at 1 atm, room air, and flowing dry nitrogen) the values of D^* were fit by an equation of the Arrhenius type with a temperature-independent preexponential factor. The values of D^* were taken as measured: they were not adjusted for the temperature variation of gas phase concentration. The fit was carried out by the method of unweighted linear least squares using $1/T$ and $\log_{10}D^*$ as the independent and dependent variables, respectively. The results, which appear in Fig. 3 along with the individual values of D^*, are

$$D^*_{\text{steam}} = 2.7\times 10^{-10\pm 0.40}e^{-(16.9\pm 1.3)\text{kcal/mol}/RT}\text{cm}^2/\text{s}, \quad (6)$$

$$D^*_{\text{room air}} = 1.3\times 10^{-12\pm 0.34}e^{-(15.5\pm 1.4)\text{kcal/mol}/RT}\text{cm}^2/\text{s}, \quad (7)$$

$$D^*_{\text{dry N}_2} = 1.8\times 10^{-13}e^{-15.7\text{kcal/mol}/RT}\text{cm}^2/\text{s}. \quad (8)$$

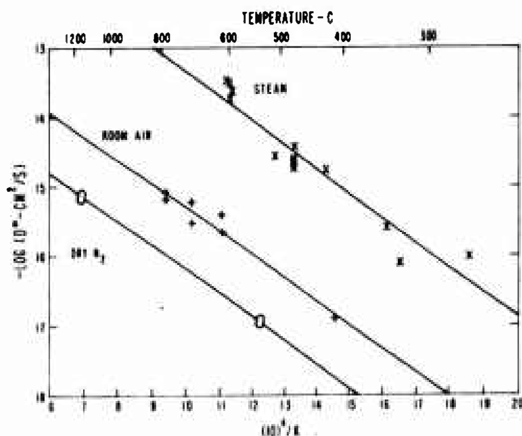

FIG. 3. Observed temperature dependence of ^{18}O tracer diffusivity at 1 atm. Solid lines represent linear least-squares fits to the data shown.

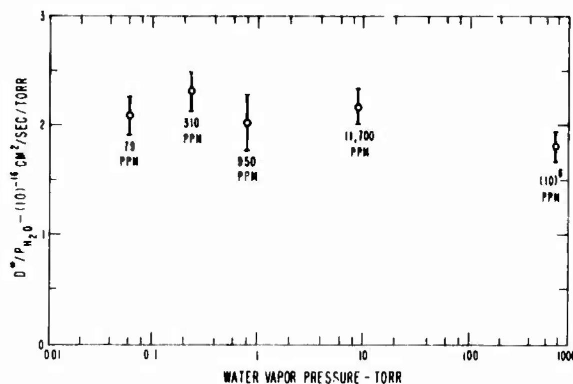

FIG. 4. Observed pressure dependence of ^{18}O tracer diffusivity in water vapor at 820 C. Labels indicate pressure in fractions of 1 atm.

The indicated errors are derived solely from the variances of the fitting parameters. The standard deviations in the fits for $\log D^*$ are 0.232 and 0.135 for steam and room air, respectively, which imply relative errors of 171% and 136% for D^*. The dry nitrogen data points fell fortuitously close; their error was not calculated. The three fitted lines shown in Fig. 3 are almost parallel; at 600 C that representing $D^*_{\text{room air}}$ lies a factor of 93 below D^*_{steam}, while $D^*_{\text{dry N}_2}$ lies a factor of 8.1 below that.

The pressure dependence of D^* was determined by calculating D^* in a similar manner for the samples heated at low pressure. As they had been heated at slightly different temperatures their values of D^* were adjusted to a common temperature (of 820 C) by assuming a temperature dependence of that seen for steam. The resulting values of D^* (per unit pressure) are displayed in Fig. 4, as is D^*_{steam} at 1 atm which was calculated using Eq. (6). The indicated errors are those arising purely from counting statistics. As can be seen, these values are consistent with a linear pressure dependence over the entire range of pressures studied.

In addition to these, measurements were made on the samples which had undergone high-vacuum treatments in order to assess substitutionality of the implanted ^{18}O and its damage to the oxide. No difference could be discerned between the alpha particle yield obtained from the sample which had been maintained at 815 C for 579 600 s at 10^{-6} Torr and that from an untreated reference sample. Another sample had its alpha particle yield measured twice. After being maintained at 690 C for 230 400 s at 10^{-6} Torr, the yield was compared to that of an untreated reference sample; again no difference could be detected. It was then maintained for 10 980 s at 1150 C in flowing dry nitrogen at 1 atm and the yield was again compared to that of reference sample; this time the results implied a value of D^* close to that of a sample which had undergone a similar treatment in dry nitrogen but had no prior vacuum treatment.

V. DISCUSSION

A. Absence of ion bombardment induced damage in SiO_2 network

To be able to compare the diffusivity measurements performed in this study to others made in SiO_2 films and

membranes, it was necessary to verify that the properties of the material used here match those of the others. For this purpose, evidence was collected which indicated that the ^{18}O implantation does not produce enough network damage to appreciably alter the oxide's structure or properties, at least as far as ^{18}O tracer diffusion is concerned.

First, the amount of ^{18}O implanted was small enough to avoid gross morphological changes brought about by its incorporation, such as blister or bubble formation. (None were seen.) The actual quantity of additional oxygen implanted in the network amounted to at most 4.2×10^{20} molecules/cm^3, which is 1.9% of the concentration of O_2 in SiO_2.[21]

Second, the shape of every observed alpha particle yield curve could be well matched to one or another of the set of theoretical curves. These were calculated on the basis of a dilute homogeneous medium; there was therefore no indication ever observed of a region of anomalous diffusivity.

Third, similar thermal treatments (in dry N_2 at 1150 C) were performed on two samples, one of which had been vacuum annealed at 690 C for 230 400 s. The ^{18}O tracer diffusivity was found to be totally unaffected by this anneal. These observations can be interpreted in the context of previous investigations of annealing of radiation damage in SiO_2.[22–25] These studies indicate that whatever damage is produced in SiO_2 is entirely removed by a 900 C inert atmosphere or vacuum anneal.[26] It is reasonable to conclude that the thermal treatments performed here to induce ^{18}O diffusion were by themselves sufficient to anneal out any damage induced by the implantation.

To verify that the proton bombardment involved in the nuclear resonance profiling did not induce any alteration of the network or diffusion of ^{18}O, alpha particle yield curves were collected in untreated reference samples both before and after lengthy proton bombardments (about 2000 μC, at a current of 0.5 μA). No difference could be detected.

Finally, to determine whether the implanted ^{18}O actually replaced existing oxygen in the network, or remained interstitial and free to migrate, an alpha particle yield curve was taken for an untreated reference sample after a high-vacuum anneal at 815 C for 579 600 s. If an appreciable amount of ^{18}O had been mobile, then it would have diffused during that period with a diffusivity characteristic of oxygen at that temperature, namely, 10^{-9} cm^2/s (Ref. 13). A calculation showed that the thermal treatment given the sample was enough to guarantee the escape of virtually all such mobile ^{18}O through the oxide surface. However, the observed yield curve was indistinguishable from that of an untreated unannealed reference sample, indicating no shift in the initial ^{18}O concentration profile. Both curves closely matched the theoretically predicted curve for such an implant, demonstrating that the initial distribution of ^{18}O formed by the implantation process consists of bound network oxygen with an insignificant fraction remaining mobile. This conclusion is in accord with studies of Al implant substitutionality in SiO_2 (Ref. 27), as well as with Primak's thermal spike model of heavy ion energy loss,[28] which predicts bond cleavage by thermal spikes involving peak temperatures of 1150 C affecting 31 000 network oxygen atoms per ion, on a time scale of 10^{-12} s; rapid refreezing ensures almost complete incorporation of implanted ^{18}O as a constituent of the network.

B. ^{18}O tracer diffusion

Once ambient water vapor was introduced, the implanted ^{18}O (which was found to be immobile in vacuum at temperatures exceeding 800 C) was seen to move in a manner consistent with its exchange with dissolved molecular water and its subsequent diffusion as a constituent of that species. This conclusion is supported by the following observations:

(i) The observed linear dependence of the ^{18}O tracer diffusivity upon ambient vapor phase concentration is identical to that expected for dissolved molecular water. This linear dependence extended over four orders of magnitude (see Fig. 4), from 1 atm to 79 ppm (of 1 atm), in pure water vapor—no carrier gases were employed. When room air was used as a carrier gas, the observed tracer diffusivity conformed to this linear dependence, but upon the partial pressure of atmospheric water. This can be seen from Fig. 3, where the measured ratio

$$D^*_{\text{steam}}/D^*_{\text{room air}} = 93$$

is close to the ratio of water vapor partial pressures for these atmospheres, namely 87 (assuming room air at 20 C and 50% relative humidity). And when samples were treated in high vacuum, no ^{18}O diffusion could be detected even after 6.7 days at 815 C.

(ii) The temperature dependence of D^*_{steam} showed an activation energy of 16.9 ± 1.3 kcal/mol, which is indistinguishable from those previously observed for water diffusion either by permeation in vitreous silica[16] or by growth rate kinetics of thermal oxidation.[4,29] These range from 16 to 18 kcal/mol. This value is clearly inconsistent with those previously observed for oxygen diffusion,[4,13,14,29,30] the most reliable of which are about 28 kcal/mol.

(iii) The magnitude of D^* is close to that expected for free exchange between network oxygen and dissolved water. In the presence of free exchange, D^* is related to D_{eff}, the experimentally measured diffusivity of water, according to Eqs. (3) and (4) by

$$(D^*/D_{\text{eff}})_{\text{free exchange}} = 15 \times 10^{-4} \text{ at } 600 \text{ C}$$
$$= 7.5 \times 10^{-4} \text{ at } 1200 \text{ C}.$$

This ratio, whose value is derived from the water solubility measurements of Moulson and Roberts (M-R),[16] can also be evaluated by using the results for D^*_{steam} obtained in this study. According to Eq. (6), this is

$$\frac{D^*_{\text{steam}}(\text{this work})}{D_{\text{eff}}(\text{M-R})} = 6.0 \times 10^{-4} \text{ at } 600 \text{ C}$$
$$= 4.4 \times 10^{-4} \text{ at } 1200 \text{ C}.$$

The magnitude of D^*_{steam} is thus seen to be consistent with free exchange at both temperatures measured by Moulson and Roberts to within a factor of 2–3, which is within the limits of accuracy obtained for the D^* measurements in this study.

(iv) In the presence of atmospheric oxygen, the activation energy for $D^*_{\text{room air}}$ remained that of water [roughly 16

kcal/mol, as indicated in Eq. (7)], rather than reverting to that of oxygen (28 kcal/mol). This was true even at 800 C, where D_{O_2} exceeds $(D_{eff})_{H_2O}$ by an order of magnitude, and even though the concentration of atmospheric oxygen was 17 times that of water vapor (20% of 760 Torr vs. 50% of 18 Torr). This implied the absence of exchange between atmospheric and network oxygen, in agreement with similar recent findings by Rosencher *et al.*,[14] who observed the failure of diffusing $^{18}O_2$ to replace existing network ^{16}O during thermal growth of oxide films on silicon in dry ^{18}O atmospheres.

In addition to supporting the above model of water diffusion in SiO_2, the measurements made in this study provided evidence indicating that chemical equilibrium between water dissolved in SiO_2 films and its reaction products occasionally had not been attained over the time spans of the thermal treatments. The values of D^* scattered in a seemingly systematic manner: the smallest values tended to be associated with the shortest thermal treatments as well as with the performance of a high-vacuum anneal prior to thermal treatment, which was done for some samples. Further, the amount of yield curve broadening in these cases was anomalously small compared to the decay in peak yield. This same phenomenon seems to have been observed in some early studies of ^{18}O permeation in SiO_2 fibers and membrances.[31] A more thorough study of the effects of nonequilibrium permeation conditions on the evolution of ^{18}O distributions is currently in progress.

VI. CONCLUSIONS

The results of the ^{18}O tracer diffusion measurements performed in this study clearly demonstrate that water diffusion in SiO_2 films proceeds by the transport of molecular water and that it is accompanied by a strong reversible reaction between molecular water and network oxygen. The observed linear dependence of tracer diffusivity upon partial pressure of atmospheric water vapor, for pressures ranging from 1 atm to as little as 0.06 Torr, indicates that network oxygen is exchanged with molecular water. The activation energy of tracer diffusion remained about 16 kcal/mol, characteristic of water diffusion, over a range of temperatures from 11[illegible]0 to 260 C. Further, the magnitude of the tracer diffusivity was consistent with the presence of free exchange between network oxygen and diffusing water. The extent of tracer diffusion proved to be unaffected by the presence of atmospheric oxygen, indicating the absence of exchange with that species. The results obtained here agreed with corresponding results obtained by most other investigators using different means. They are in complete agreement with recently proposed models of oxygen and water diffusion in SiO_2 in which the diffusion proceeds by transport of the molecular species through interstices in the network without any direct reaction between the molecular species and the SiO_2 (the strong exchange reaction accompanying water diffusion involves immobile OH groups which are dissociation products of the molecular water).

The process employed for introducing tracer ^{18}O into the network, that of ion implantation, was shown to produce a region within the oxide in which the ^{18}O was fully incorporated in the network: no ^{18}O diffusion was observed in high vacuum, even after 161 h at 815 C. The properties of the network remained otherwise unaltered, at least as far as diffusion was concerned. This was demonstrated both by the close match of the data to theoretical predictions based on a dilute homogeneous medium as well as by the absence of any effect on diffusion of a high-temperature treatment which was sufficient to anneal out any implantation-induced damage. These findings indicate that the thermal treatments performed to induce ^{18}O diffusion were themselves sufficient to anneal out any damage.

The technique of nuclear resonance profiling proved to be a convenient, nondestructive, and sensitive method of measuring ^{18}O diffusivities as low as 10^{-17} cm^2/s at temperatures as low as 260 C.

ACKNOWLEDGMENTS

The authors wish to express gratitude to S. Kronenberg and J. Kohn for their persistent support, to G. Brucker and F. Kolondra of RCA Labs, Princeton, for performing the ion implantation, to E. Ahlstrom for preparing the thermal oxides, to A. Hager for glass fabrication, and particularly to H. Berkowitz for advice on theory and on programming, and R. Lux for his invaluable and generously provided cooperation, both in the nuclear profiling and in discussions of physical mechanisms.

APPENDIX. CONSTITUENT FUNCTIONS OF THE ALPHA PARTICLE YIELD INTEGRAL

$\rho(x,t)$: The SiO_2 film is assumed to be a dilute homogeneous medium with respect to water diffusion; the concentrations of dissolved molecular water and reacted water remain at their equilibrium levels. If the film is heated for a duration t under those conditions, then the distribution $\rho(x,t)$ of ^{18}O in excess of the natural background level of 0.02% isotopic fraction will change with time so as to satisfy the diffusion equation

$$\dot{\rho}(x,t) = D^* \frac{\partial^2}{\partial x^2} \rho(x,t),$$

with D^* independent of ρ, x, and t. The ^{18}O is assumed to be transported only as a constituent of molecularly dissolved water. The boundary conditions are therefore determined by considering the behavior of this substance at the boundaries.

(i) At the oxide surface, equilibrium between the outside atmosphere and water dissolved in the oxide occurs rapidly; surface absorption and reactions are not involved (Ref. 12, p. 128). This implies the condition $\rho(0,t) = 0$.

(ii) At the oxide-silicon interface, the boundary condition is temperature dependent. This can be seen from the analysis of steady-state steam oxidation performed by Deal and Grove.[4] According to their Eqs. (6) and (7), the ratio of molecularly dissolved water concentration at the interface to that at the outer surface is given by

$$\frac{C_i}{C_0} = \frac{1}{1 + kx_0/D_{eff}},$$

where k, the interface rate constant, is determined through

observations of the linear and parabolic rate constants A and B and the equilibrium solubility C^* (x_0 is the layer thickness). Deal and Grove give a value of

$$k = 1.8\times 10^3\ \mu\text{m/h}$$

at 1000 C with an activation energy of 45.3 kcal/mol. Using this in conjunction with the Moulson and Roberts equation[16]

$$D_{\text{eff}} = 10^{-6}\exp[-18.3(\text{kcal/mol})/RT], \quad (\text{cm}^2/\text{sec})$$

the temperature dependence of C_i/C_0 is seen to be the following:

T(C)	kx_0/D_{eff}	C_i/C_0
250	3.1×10^{-7}	~ 1
475	7.7×10^{-4}	~ 1
600	0.011	0.989
1000	1.4	0.417
1200	5.9	0.145

At temperatures encountered in this work, the ratio C_i/C_0 is more than 98%. The appropriate boundary condition is therefore $\partial\rho(x_0,t)/\partial x = 0$.

(iii) For sufficiently long times all the excess ^{18}O will eventually disappear, either through surface leakage or interface incorporation of diffusing molecular water, implying the condition $\rho(x,\infty) = 0$.

(iv) The initial distribution $\rho(x,0)$ was taken to be that implantation profile given by Gibbons *et al.*[17] for the appropriate experimental conditions. This was an Edgeworth distribution with a mean projected range of 768 Å, a standard deviation of 283 Å, and a third moment ratio of -0.163. The solution to the diffusion equation is straightforward, being

$$\rho(x,t) = \sum_{n=1}^{\infty} B_{2n-1} e^{-[(2n-1)(\pi/2x_0)]^2 D^* t} \sin\left(\frac{2n-1}{2}\frac{\pi}{x_0}x\right),$$

with

$$B_k = 2\int_0^1 dx\, \sin(\tfrac{1}{2}k\pi x)\rho(x,0).$$

$g(E_b,E_i)$: The distribution of energies in the incident beam was found experimentally through analysis of the thick-target ^{27}Al$(p,\gamma)^{28}$Si excitation curve. The energy spread amounted to less than 1 keV; the shape was taken to be a Gaussian with a standard deviation of 1 keV.

$f(E,E_i,x)$: After some test calculations with Vavilov distributions[32] it was found that for the particular conditions of this experiment a sufficiently accurate approximation to the energy straggling distribution was

$$f(x,\Delta) = (2\pi k_s x)^{-1/2}\exp[-(\Delta - \epsilon x)^2/2k_s x],$$

where $\Delta = E_i - E(x)$, $k_s = 17.75\ \text{keV}^2\,\mu\text{m}^{-1}$ (Ref. 33), and $\epsilon = 61\ \text{keV}\,\mu\text{m}^{-1}$ (Ref. 18).

$d\sigma/d\Omega(E)$: The recent data of Amsel *et al.* (Ref. 34, p. 163) in the region of the 629-keV resonance was well fit by a sum of two interfering Lorentzians plus an exponential background:

$$\frac{d\sigma}{d\Omega}(E) = \frac{\tfrac{1}{4}\Gamma_{\text{res}}^2(12.78 - K) - (E - E_{\text{res}})4.7e^{(E - E_{\text{res}})}}{(E - E_{\text{res}})^2 + \tfrac{1}{4}\Gamma_{\text{res}}^2} + Ke^{(E - E_{\text{res}})/58}\ \text{mb/steradian},$$

where

$$K = 2 \quad (E < E_{\text{res}})$$
$$= 1.75 \quad (E > E_{\text{res}}),$$
$$\Gamma_{\text{res}} = 1.9\ \text{keV},$$
$$E_{\text{res}} = 629\ \text{keV}.$$

[1] H. Agajanian, Solid State Technol. **19**, 36 (1977).
[2] R. H. Doremus, in *Reactivity of Solids*, edited by Mitchell, de Vries, Roberts, and Cannon (Wiley, New York, 1969), p. 667.
[3] G. Amsel, J. P. Nadai, E. D'Artemaire, D. David, E. Girard, and J. Moulin, Nucl. Instrum. Methods **92**, 481 (1971).
[4] B. E. Deal and A. S. Grove, J. Appl. Phys. **36**, 3770 (1965).
[5] M. B. Brodsky and D. Cubicciotti, J. Am. Chem. Soc. **73**, 3497 (1951).
[6] R. H. Doremus, J. Phys. Chem. **80**, 1773 (1976).
[7] E. P. EerNisse, J. Appl. Phys. **45**, 167 (1974).
[8] A. N. Knopp and R. Stickler, Electrochem. Technol. **5**, 37 (1967).
[9] N. Nagasima, Jpn. J. Appl. Phys. **9**, 879 (1970).
[10] O. L. Anderson and D. A. Stuart, J. Am. Ceram. Soc. **37**, 573 (1964).
[11] M. E. Milberg, in *Fast Ion Transport in Solids*, edited by W. Van Gool (North Holland, Amsterdam, 1973), p. 378.
[12] R. H. Doremus, *Glass Science* (Wiley, New York, 1973).
[13] F. J. Norton, Nature **191**, 701 (1961).
[14] E. Rosencher, A. Straboni, S. Rigo, and G. Amsel, Appl. Phys. Lett. **34**, 254 (1979).
[15] J. F. Shackelford and J. S. Masaryk, J. Noncryst. Solids **21**, 55 (1976).
[16] J. Moulson and J. P. Roberts, Trans. Faraday Soc. **57**, 1208 (1961).
[17] J. F. Gibbons, W. S. Johnson, and S. W. Mylroie, *Projected Range Statistics*, 2nd Ed. (Academic, New York, 1975).
[18] E. Bonderup and P. Hvelplund, Phys. Rev. A **4**, 562 (1971).
[19] K. L. Dunning, G. K. Hubler, J. Comas, W. H. Lucke, and H. L. Hughes, Thin Solid Films **19**, 145 (1973).
[20] A number of computations preceded the calculation of the yield curves: these involved determining the appropriate values of the constants appearing in the formulas for the reaction cross section, the beam energy spread and the initial ^{18}O distribution in Appendix. Although approximate values of the constants were available from the sources cited here, the final values were determined by finding the best match of the calculatd initial yield curve (topmost curve in Fig. 4), to the observed yield curve of a reference sample. The goodness of fit can be judged by inspection of the topmost curve in Fig. 2.
[21] A. S. Grove, *Physics and Technology of Semiconductor Devices* (Wiley, New York, 1967).
[22] V. Antonini, A. Manara, and P. Lensi, in *The Physics of* SiO_2 *and its Interfaces*, edited by S. Pantelides (Pergamon, New York, 1978).
[23] A. Monfret and J. Bernard, in *Proceedings of the 2nd International Conference on Ion Implantation in Semiconductors*, edited by I. Ruge and J. Graul (Springer-Verlag, Berlin, 1971).
[24] S. Wang, T. Russell, and B. S. H. Royce, PSSL Report No. 300874, Princeton University, 1974 (unpublished).
[25] E. P. EerNisse and C. B. Norris, J. Appl. Phys. **45**, 5196 (1974).
[26] G. H. Sigel (private communication).
[27] D. J. DiMaria, D. R. Young, W. R. Hunter, and C. M. Serrano, IBM J. Res. Dev. **22**, 289 (1978).
[28] W. Primak, J. Appl. Phys. **43**, 2745 (1972).
[29] A. G. Revesz and R. J. Evans, J. Phys. Chem. Solids **30**, 551 (1969); Y. Ota and S. R. Butler, J. Electrochem. Soc. **121**, 1107 (1974); E. A. Irene and R. Ghez, J. Electrochem. Soc. **124**, 1757 (1977), E. Ehara, K. Sakuma, and K. Ohwada, J. Electrochem. Soc. **126**, 2249 (1979).
[30] E. A. Irene, J. Electrochem. Soc. **121**, 1613 (1974); M. A. Hopper, R. A. Clarke, and L. Young, *ibid.* **122**, 1216 (1975); B. E. Deal, D. W. Hess, J. D. Plummer, and C. P. Ho, *ibid.* **125**, 339 (1978).
[31] R. Haul and G. Dumbgen, Z. Electrochem. **66**, 636 (1962); E. L. Williams, J. Am. Ceram. Soc. **48**, 190 (1965).
[32] P. V. Vavilov, Soviet Phys. JETP **5**, 749 (1957).
[33] U. Fano, Ann. Rev. Nucl. Sci. **13**, 1 (1963).
[34] *Ion Beam Handbook for Materials Analysis*, edited by J. W. Mayer and E. Rimini (Academic, New York, 1977).